Assumed-Mode-Based Dynamic Model for Cable Robots with Non-straight Cables

Jorge Ivan Ayala Cuevas[1], Édouard Laroche[2(✉)], and Olivier Piccin[3]

[1] INSA of Strasbourg, Strasbourg, France
jorge.ayalacuevas@insa-strasbourg.fr

[2] ICube Laboratory, Strasbourg University, Strasbourg, France
laroche@unistra.fr

[3] ICube Laboratory, INSA of Strasbourg, Strasbourg, France
olivier.piccin@insa-strasbourg.fr

Abstract. This paper presents an original method for deriving models of flexible cable robots including cable sagging based on assumed mode assumption. This method allows to derive low-order models that specially suit for control applications. The case of a winder and a planar cable without elongation but with sagging in the plane of movement is first considered. Then, the model of a planar robot with a punctual platform with three cables is presented. The model is written in the Lagrange framework for constrained systems. Simulation results for a three-cable robots are presented and discussed.

1 Introduction

Cable-driven parallel robots (CDPR) are a special class of parallel manipulators in which the end-effector is connected to the base through cables, the movement being provided by the winding and unwinding of cables. Compared to conventional serial or parallel manipulators, CDPR have interesting features: a large workspace capability, low inertia of moving components and reduced obstruction of the workspace. Their main drawback is common to all flexible manipulators in which the deflections and elongation of the links limit the precision when determining the position of the end-effector from the measurements of the joint positions.

A number of approaches considers straight inextensible cables [3,5]. Straight massless extensible cables are also often considered. In a simplistic case, the cable is modeled as the association of a rigid link with a spring which stiffness is inversely proportional to the cable length [8,13]. Models from continuum mechanics are also available in the literature that provide more accurate models of elastic cables [11]. When the mass of the cable is not negligible anymore, the sagging effect must be accounted for. In statics, this effect results in the catenary equation and is well documented [7,14]. Finite-element models are available for but they have the drawback of resulting in high order models [4]. More recently, Arsenault [2] and Yuan *et al.* [15] have considered elastic cables with sagging.

C. Gosselin et al. (eds.), *Cable-Driven Parallel Robots*,
Mechanisms and Machine Science 53, DOI 10.1007/978-3-319-61431-1_2

Following the dynamic stiffness matrix method [1], the stiffness matrix is first determined in statics and then introduced in the dynamic model.

The key idea of the original approach proposed herein is to consider cables as particular cases of flexible segments. When considering the control of systems composed of deformable segments modeled as Euler-Bernoulli beams, the assumed-mode approach is certainly the most standard and has been intensively used for serial robots [9,10]. The segment deformations are first written as sums of contributions of a given base. Then, the geometry can be written as a function of a generalized position vector that includes deformation variables. The dynamic model, given by the Lagrange equation of motion in a standard way, accounts for the kinetic energy of the cable displacements. In this contribution, this approach is considered in which deformable segments are replaced by perfectly flexible and inextensible cables. As an illustrative example, the case of a planar robot with a punctual platform, actuated by three or more cables, is considered. Cables are assumed to be affected by sagging in the plane of movement.

In Sect. 2, the model of a single cable and its winder, undergoing transverse deformation in a plane is considered. Based on Lagrange approach, a dynamic model is derived. In Sect. 3, the model of a planar robot with three or more cables is considered. The DAE model is developed and then reduced. In Sect. 4, some simulation results are presented and discussed. The model derived with Maple and the simulation with Matlab-Simulink are available online[1].

2 Single Cable Modeling

In this section, we focus on the an elementary constitutive element of the planar robot depicted in Fig. 2, namely, one single cable winded at one side and submitted at the other side to an external force.

2.1 Single Cable Modeling

Up to four deformation fields can be considered when modeling a deformable beam under Euler-Bernoulli assumption [12]. Herein, the cable subjected to sagging is considered as a perfectly flexible and inextensible 1-dimensional body. In the current study, the only deformation field of interest is the transverse deformation in the plane of motion. The final geometry of the cable will be given as the composition of three steps: unwinding, shaping and rotation.

Let us consider a single cable $\#k$ operated by a winder $\#k$. The cable is tangent to the winder at point W_k and has an end-point denoted P_k. The unwinded portion of the cable is the planar curve between W_k and P_k of length l_k. Let $\mathscr{F}_b = (O_b, \mathbf{x_b}, \mathbf{y_b})$ and $\mathscr{F}_k = (W_k, \mathbf{x_k}, \mathbf{y_k})$ denote respectively the fixed global reference frame and the local reference frame attached to the winder $\#k$. The position of W_k and the orientation of the cable at W_k are defined by (x_{W_k}, y_{W_k}) and φ_k respectively as indicated in Fig. 1.

[1] http://icube-avr.unistra.fr/fr/index.php/Planar_cable_robot_with_non_straight_cables.

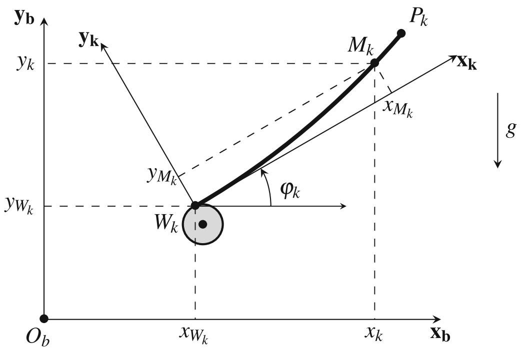

Fig. 1. General configuration of a single cable.

From an initial configuration where the cable is straight along the $\mathbf{x_k}$ direction, let us now consider a small displacement of the cable that alters the cable shape but preserves its point of tangency W_k on the winder. In this elementary displacement, a point of coordinates $(x, 0)$ with $x \in [0, l_k]$ is moved to the point M_k of coordinates $(x_{M_k} = x + \delta x_{M_k}, y_{M_k} = \delta y_{M_k})$ in the local frame $\mathscr{F}_k$. Finally, the coordinates (x_k, y_k) of the point M_k expressed in the global frame $\mathscr{F}_b$ can be obtained using an homogeneous transformation as

$$\begin{bmatrix} x_k \\ y_k \\ 1 \end{bmatrix} = \begin{bmatrix} \cos\varphi_k & -\sin\varphi_k & x_{W_k} \\ \sin\varphi_k & \cos\varphi_k & y_{W_k} \\ 0 & 0 & 1 \end{bmatrix} \begin{bmatrix} x_{M_k} \\ y_{M_k} \\ 1 \end{bmatrix}. \tag{1}$$

Notice that if the cable is inextensible, the small displacement variables are linked by

$$\left(\frac{\partial \delta x_{M_k}}{\partial x} + 1\right)^2 + \left(\frac{\partial \delta y_{M_k}}{\partial x}\right)^2 = 1 \tag{2}$$

and assuming that $\left|\frac{\partial \delta y_{M_k}}{\partial x}\right| \ll 1$, Eq. (2) yields

$$\delta x_{M_k}(x,t) = -\frac{1}{2}\int_0^x \left(\frac{\partial \delta y_{M_k}(u,t)}{\partial u}\right)^2 \mathrm{d}u. \tag{3}$$

The small displacement δy_{M_k} along the $\mathbf{y_k}$ direction is assumed to be the sum of a number of contributions that can be written, with a given basis $\Phi_k(x)$ truncated at the order N, as

$$\delta y_{M_k}(x,t) = \sum_{j=1}^{N} \Phi_j(x)\, V_{jk}(t) \tag{4}$$

where V_{jk} is the generalized coordinate for mode Φ_j. In the sequel, we choose to work with a polynomial basis of the form $\Phi_j(x) = x^{j+1}$. In this assumed mode approach, other basis could have been used, as for example the set of modal deformations described in [9].

Upon substitution of the coordinates (x_{M_k}, y_{M_k}) into Eq. (1), the position of a point M_k in the global reference frame can be readily calculated as analytic functions, namely, $x_k(\tilde{q}_k)$ and $y_k(\tilde{q}_k)$ with $\tilde{q}_k = \left[x\ V_{1k}\ \ldots\ V_{Nk}\ \varphi_k\right]^T$. At this point, when x is set to the unwinded length of cable l_k, the model of the single cable can be parameterized by the generalized coordinate vector $q_k = \left[l_k\ V_{1k}\ \ldots\ V_{Nk}\ \varphi_k\right]^T$ containing $N+2$ independent parameters q_{k_i}.

2.2 Cable Dynamic Model

Based on the parameterization presented in the previous subsection, a dynamic model of a single cable is now introduced as a basic example of the approach. The details of the three-cable robot are not given in the paper but are available online (see the link given at the first page).

The cable is winded at one side with a fixed winder actuated by a torque τ_k and is subject to the gravitational acceleration $-g\mathbf{y_b}$. The other end P_k is submitted to an arbitrary force $\mathbf{F_k}$ which coordinates in $\mathscr{F}_b$ are (F_{x_k}, F_{y_k}). The cylindric winder is of radius R and inertia J_0. The cable has a linear density ρ and a total length l_t. Accounting for the wounded portion of the cable, the actual inertia is $J_k = J_0 + \rho(l_t - l_k)R^2$. Furthermore, the winder angular position θ_k is related to the unwinded length of cable l_k by $l_k = -R\theta_k$. The gravitational potential energy of the single cable writes

$$V_k = \int_0^{l_k} \rho\, g\, y_k(\tilde{q}_k)\, \mathrm{d}x. \tag{5}$$

The kinetic energy of the single cable and its rotating winder writes

$$T_k = \frac{1}{2}\frac{J_k}{R^2}\dot{l}_k^2 + \frac{1}{2}\int_0^{l_k} \rho\left(\dot{x}_k(\tilde{q}_k)^2 + \dot{y}_k(\tilde{q}_k)^2\right)\mathrm{d}x \tag{6}$$

in which the velocity terms $\dot{x}_k(q_k)$ and $\dot{y}_k(q_k)$ can be calculated as $\displaystyle\sum_{i=1}^{N+2}\frac{\partial x_k}{\partial q_{k_i}}\dot{q}_{k_i}$ and $\displaystyle\sum_{i=1}^{N+2}\frac{\partial y_k}{\partial q_{k_i}}\dot{q}_{k_i}$. The kinetic energy can then be written under its quadratic form $T_k = \frac{1}{2}\dot{q}_k^{\mathrm{T}} M_k(q_k)\, \dot{q}_k$ where $M_k(q_k)$ refers to the kinetic energy matrix. The Lagrange's equations of motion can be written as

$$\frac{\mathrm{d}}{\mathrm{d}t}\frac{\partial T_k}{\partial \dot{q}_k} - \frac{\partial T_k}{\partial q_k} = \mathit{\Gamma}_k\, Q_k - \frac{\partial V_k}{\partial q_k} \tag{7}$$

where $\mathit{\Gamma}_k = \left[F_{x_k}\ F_{y_k}\ \tau_k\right]$ corresponds to the actions applied on the system and Q_k a matrix of partial velocity terms, relative to the generalized coordinates and determined from the virtual-work principle as:

$$Q_k = \begin{bmatrix} \frac{\partial x_{P_k}}{\partial q_{k_1}} & \frac{\partial x_{P_k}}{\partial q_{k_2}} & \dots & \frac{\partial y_{P_k}}{\partial q_{k_{N+2}}} \\ \frac{\partial y_{P_k}}{\partial q_{k_1}} & \frac{\partial y_{P_k}}{\partial q_{k_2}} & \dots & \frac{\partial x_{P_k}}{\partial q_{k_{N+2}}} \\ -\frac{1}{R} & 0 & \dots & 0 \end{bmatrix} \tag{8}$$

where x_{P_k} and y_{P_k} denote the position functions of the point P_k at which the effort $\mathbf{F_k}$ is applied. The entries of the $1 \times (N+2)$ line matrix $\Gamma_k\, Q_k$ correspond to the generalized forces acting on the cable.

Denoting $p_k = \dfrac{\partial T_k}{\partial \dot{q}_k} = \dot{q}_k^{\mathrm{T}}\, M_k$, the line matrix of generalized momentum, the model can be rewritten under the following state-space representation:

$$\dot{p}_k = C_k + \Gamma_k\, Q_k - G_k \tag{9}$$

$$\dot{q}_k = M_k^{-1}\, p_k^{\mathrm{T}} \tag{10}$$

where

$$C_k = \frac{\partial T_k}{\partial q_k} = \left[\tfrac{1}{2}\dot{q}_k^{\mathrm{T}} \tfrac{\partial M_k}{\partial q_{k_1}} \dot{q}_k \;\dots\; \tfrac{1}{2}\dot{q}_k^{\mathrm{T}} \tfrac{\partial M_k}{\partial q_{k_{N+2}}} \dot{q}_k\right] \tag{11}$$

$$G_k = \frac{\partial V_k}{\partial q_k} = \left[\tfrac{\partial V_k}{\partial q_{k_1}} \;\dots\; \tfrac{\partial V_k}{\partial q_{k_{N+2}}}\right] \tag{12}$$

3 Planar Robot with n cables

A planar cable robot operated by several cables is now considered as presented in Fig. 2. Its platform is considered as a punctual mass m located at point P of coordinates (x_P, y_P) in the global reference frame. The number of cables in this example is three but the presented method is applicable to any number of cables.

3.1 Dynamic Model

The generalized coordinate vector q for the system includes the two parameters of the mobile platform and the n sets of parameters relative to each cable. The column vector q can be written symbolically as

$$q = \left[x_P\ y_P\ q_1^{\mathrm{T}} \dots q_n^{\mathrm{T}}\ \right]^{\mathrm{T}} \tag{13}$$

which corresponds to $n(N+2)+2$ non independent parameters.

The total kinetic energy is calculated as the sum of contributions of each cable plus the platform of mass m, yielding to $T = \frac{1}{2}\dot{q}^{\mathrm{T}} M\, \dot{q}$ with $M = \mathrm{diag}(M_0, M_1, \dots, M_n)$ where $M_0 = \mathrm{diag}(m, m)$ is the kinetic inertia matrix of the platform and M_k, $k = 1, ..., n$ denotes the kinetic inertia matrix for cable $\#k$.

With the selected generalized coordinate vector q and gathering the terms $\Gamma_k Q_k$ corresponding to each cable, the generalized force vector acting on the system writes

$$\Gamma Q = \left[F_{x_P}\ F_{y_P}\ \Gamma_1 Q_1 \dots \Gamma_n Q_n\right] \tag{14}$$

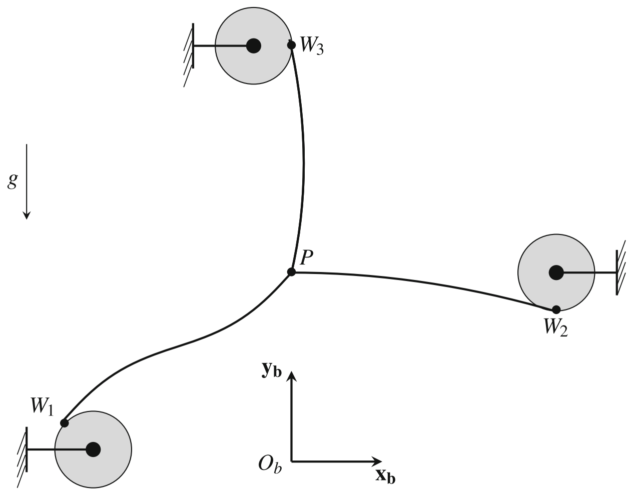

Fig. 2. Schematics of a planar cable robot with 3 cables.

where F_{x_P} and F_{y_P} are the components, in the global reference frame, of an effort $\mathbf{F_P}$ acting on the moving platform at point P. The gravitational potential energy for the whole system can be calculated as $V = \sum_{k=1}^{n} V_k - mgy_P$. In the sequel, we assume that $\mathbf{F_P} = \mathbf{0}$.

The coincidence of the positions of the platform with the cable ends provide $h = 2n$ geometric (holonomic) constraints of the form $h_r(q) = 0$, $r = 1, \ldots, h$:

$$h_{2k-1} = x_{P_k}(q_k) - x_P \tag{15}$$

$$h_{2k} = y_{P_k}(q_k) - y_P \tag{16}$$

with $k = 1, \ldots, n$.

As the $n(N+2)+2$ parameters are related by the h geometric constraints (15) and (16), the dynamic behavior of the system can be obtained using Lagrange's equations with h multipliers [6]. Upon differentiation with respect to time, the constraint relations can be written $A(q)\,\dot{q} = 0$ where A is the Jacobian of the constraints with respect to the generalized coordinate vector q whose entries write $A_{rk}(q) = \frac{\partial h_r(q)}{\partial q_k}$.

Using $\lambda = \left[\lambda_1 \ldots \lambda_h\right]^{\mathrm{T}}$ as the column vector of the Lagrange multipliers, the Lagrange's equations can be written as:

$$\frac{\mathrm{d}}{\mathrm{d}t}\frac{\partial T}{\partial \dot{q}} - \frac{\partial T}{\partial q} = \Gamma\, Q - G + \lambda^{\mathrm{T}} A \tag{17}$$

with $G = \frac{\partial V}{\partial q}$. Given that the generalized momentum matrix $p = \dfrac{\partial T}{\partial \dot{q}} = \dot{q}^{\mathrm{T}}\, M$ and after differentiation of the geometric constraints, the differential-algebraic equations of the system can be obtained as

$$\begin{bmatrix} M & -A^{\mathrm{T}} \\ A & 0 \end{bmatrix} \begin{bmatrix} \ddot{q} \\ \lambda \end{bmatrix} = \begin{bmatrix} C^{\mathrm{T}} + (\Gamma Q)^{\mathrm{T}} - G^{\mathrm{T}} - \dot{M}\dot{q} \\ -\dot{A}\dot{q} \end{bmatrix}. \tag{18}$$

Since the equations set (18) is linear with respect to $\ddot{q}$ and λ, solving for $\ddot{q}$ can be done directly by inversion of the matrix $\begin{bmatrix} M & -A^{\mathrm{T}} \\ A & 0 \end{bmatrix}$ either online, numerically or offline, using a computer algebra system.

4 Simulation Results

A system composed of three cables and three winders evenly distributed on a circle with a 10 m diameter has been tested with the following set of parameters: $l_t = 5$ m, $\rho = 0.2$ kg/m, $R = 0.1$ m, $J_0 = 2.5 \cdot 10^{-3}$ kg·m^2 and $m = 1$ kg. The cable models have been set with one mode ($N = 1$).

A controller has been implemented in order to have the platform follow a desired trajectory (x^*, y^*). A number of approaches are available in the literature for cable robot control [3,8,13]. Herein, a simplistic approach is used, assuming that both position and speed of the platform are available.

The controller has been established on the kinetic model $\dot{\theta} = J(q_0)\,\dot{q}_0$ that connects the vector of the angular velocities $\dot{\theta}$ to the velocity of the platform $\dot{q}_0$ through the Jacobian matrix $J(q_0)$, assuming straight cables. The control signals (i.e. the motor torques) are computed as

$$u = u_0 \begin{bmatrix} 1 \\ 1 \\ 1 \end{bmatrix} + J^{\mathrm{T}\dagger}(q_r) \begin{bmatrix} u_x \\ u_y \end{bmatrix} \tag{19}$$

where u_0 ensures a positive tension in the cables; $J^{\mathrm{T}\dagger}$ is the pseudo-inverse of the transpose of J; u_x and u_y are the control actions in the (x, y) plane, computed with a proportional-derivative (PD) control law given in the Laplace domain:

$$u_x(s) = K(s)\,(x^*(s) - x(s)) \tag{20}$$

$$u_y(s) = K(s)\,(y^*(s) - y(s)) \tag{21}$$

where s denote the Laplace variable and $u_x(s)$ is the signal u_x in the Laplace domain. The same PD controllers with filtering are used for both x and y directions:

$$K(s) = K_p + K_d \frac{\omega_f\, s}{\omega_f + s} \tag{22}$$

where the coefficients have been chosen as following: the proportional gain is $K_p = 400$ N; the derivative gain is $K_d = 100$ N.s; the filtering frequency is $\omega_f = 100$ rad/s.

The robot being initialized at the center of the workspace without sagging, the reference remains at the center during 2 s before moving by 1 m along the $\mathbf{x_b}$ direction, then following a square of 2 m side length centered in the workspace at a constant speed of 1 m/s and finally coming back to the origin. The reference signals and the actual trajectory can be seen in Fig. 3. The reference trajectory is tracked with some oscillations. One can check in Fig. 4 that the tensions remain positive during operation. In Fig. 5, the actual trajectory is presented in the $(\mathbf{x_b}, \mathbf{y_b})$ plane and the geometry of the cables is plotted for three positions in order to see how sagging evolves dynamically at a fast pace. The modal coordinates V_{11}, V_{12} and V_{13} are presented in Fig. 6. One can see how they vary in term of amplitude and frequency. Notice that the sagging at rest observed at $t = 2$ s is reduced compared to the variations observed during dynamic operation.

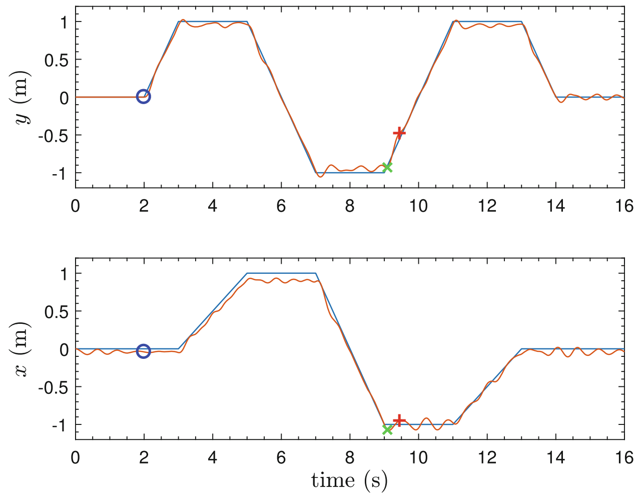

Fig. 3. Trajectory of the effector with respect to time: reference and actual position.

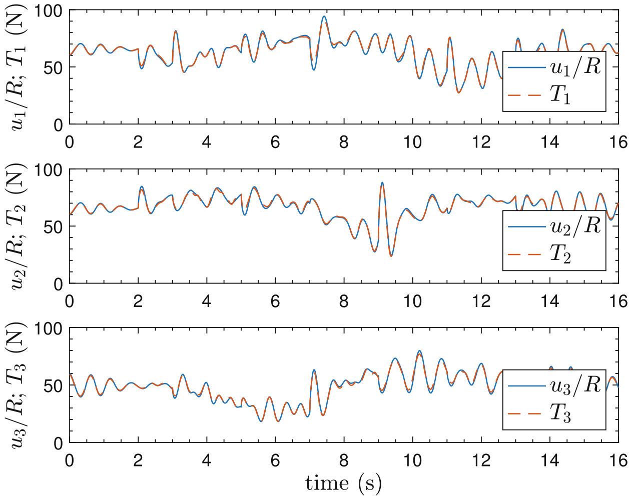

Fig. 4. Evolution of the cable tensions T_k and of the control signals u_k.

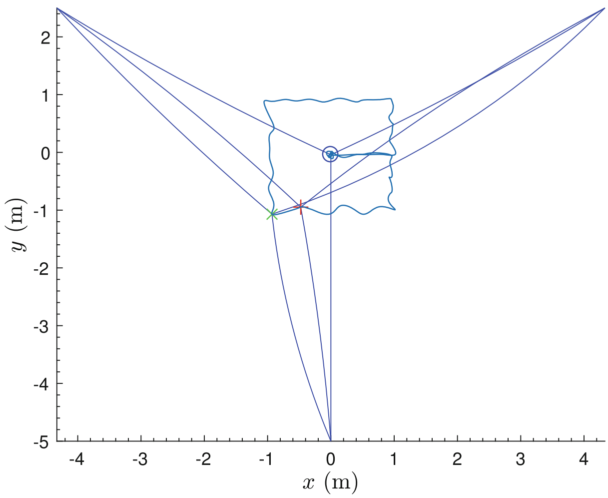

Fig. 5. Trajectory of the effector in the x-y plan and geometry of the cables at $t = 2$ s; 9.1 s and 9.45 s.

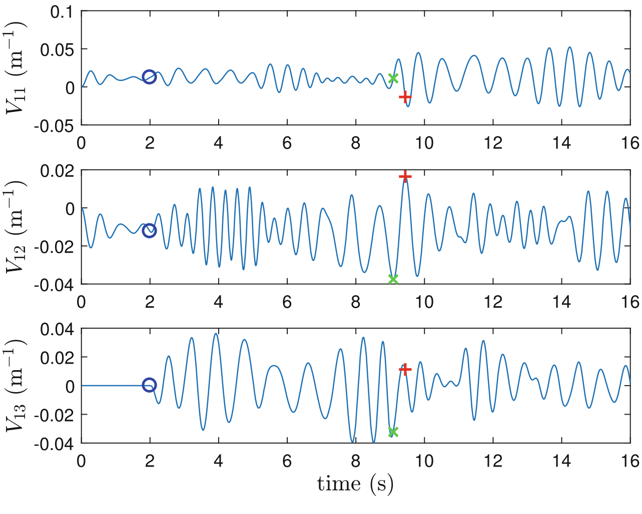

Fig. 6. Evolution of the deformation variables V_{1k} with respect to time.

In order to highlight the effect of the cable dynamics on the trajectories, the trajectories obtained for two different values of the linear density of the cables are given in Fig. 7. For a low linear density ($\rho = 0.02$ kg/m), the reference is quite well tracked whereas the dynamic behavior of the cables observed for $\rho = 0.2$ kg/m significantly degrades the system behavior.

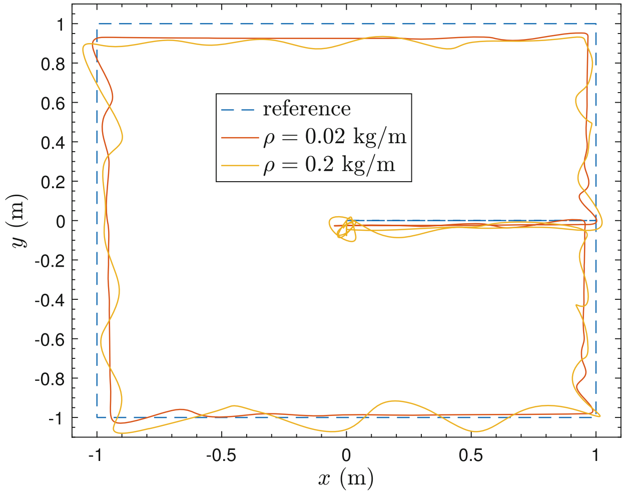

Fig. 7. Trajectories of the effector in the x-y plane for different values of ρ.

5 Conclusion

In this paper, an original approach has been proposed to account for the cable movements for very dynamic operations of CDPR. Using the assumed deformation method, a dynamic model is derived using the Lagrange's equations of motion for constrained systems. The method has been implemented in the case of a planar CDPR with three cables. Simulation results have shown the effect of the cable movements on the system behavior.

The next steps to further assess the method's efficiency will include comparisons of the obtained simulation results with experimental data as well as with other available approaches. Another perspective will consist in extending the model to account for the cable elongation in the planar case but also in the more challenging case of 3D setups.

References

1. Ansell, A.: The dynamic element method for analysis of frame and cable type structures. Eng. Struct. **27**(13), 1906–1915 (2005)
2. Arsenault, M.: Stiffness analysis of a planar 2-dof cable-suspended mechanism while considering cable mass. In: First International Conference on Cable-Driven Parallel Robots, Stuttgart, Germany (2012)
3. Chellal, R., Cuvillon, L., Laroche, E.: Model identification and vision-based H_∞ position control of 6-dof cable-driven. Int. J. Control **90**(4), 684–701 (2017)
4. Du, J., Ding, W., Bao, H.: Cable vibration analysis for large workspace cable-driven parallel manipulators. In: First International Conference on Cable-Driven Parallel Robots, Stuttgart, Germany (2012)

5. Gosselin, C.: Global planning of dynamically feasible trajectories for three-dof spatial cable-suspended parallel robots. In: First International Conference on Cable-Driven Parallel Robots, Stuttgart, Germany (2012)
6. Greenwood, D.T.: Advanced Dynamics. Cambridge University Press, Cambridge (2003)
7. Irvine, H.M.: Cable Structures. MIT Press, Cambridge (1981)
8. Khosravi, M.A., Taghirad, H.D.: Dynamic modeling and control of parallel robots with elastic cables: singular perturbation approach. IEEE Trans. Rob. **30**(3), 694–704 (2014). doi:10.1109/TRO.2014.2298057
9. De Luca, A., Siciliano, B.: Closed-form dynamic model of planar multilink lightweight robots. IEEE Trans. Syst. Man Cybern. **21**(4), 826–839 (1991)
10. De Luca, A., Siciliano, B.: Inversion-based nonlinear control of robot arms with flexible links. AIAA J. Guidance Control Dyn. **16**(6), 1169–1176 (1993)
11. Nguyen, T.T., Laroche, E., Cuvillon, L., Gangloff, J., Piccin, O.: Identification du modèle phénoménologique d'un robot parallèle à câbles. J. Européen des Systémes Automatisès **46**(6–7), 673–689 (2012)
12. Shi, P., McPhee, J., Heppler, G.: A deformation field for Euler-Bernouilli beams with application to flexible multibody dynamics. Multibody Syst. Dyn. **5**(1), 79–104 (2001)
13. Weber, X., Cuvillon, L., Gangloff, J.: Active vibration canceling of a cable-driven parallel robot in modal space. In: IEEE International Conference on Robotics and Automation, Seattle, WA, USA, pp. 1599–1604 (2015)
14. Yao, R., Li, H., Zhang, X.: A modeling method of the cable driven parallel manipulator for fast. In: First International Conference on Cable-Driven Parallel Robots, Stuttgart, Germany (2012)
15. Yuan, H., Courteille, E., Deblaise, D.: Static and dynamic stiffness analyses of cable-driven parallel robots with non-negligible cable mass and elasticity. Mech. Mach. Theory **85**, 64–81 (2015)

Springer

http://www.springer.com/978-3-319-61430-4

Cable-Driven Parallel Robots
Proceedings of the Third International Conference on Cable-Driven Parallel Robots
Gosselin, C.; Cardou, P.; Bruckmann, T.; Pott, A. (Eds.)
2018, XII, 416 p. 221 illus., Hardcover
ISBN: 978-3-319-61430-4